Coherent exciton dynamics in nanocrystal chain arrays

Suc-Kyoung Hong and Seog Woo Nam
Department of Display and Semiconductor Physics, Korea University, Seochang, Jochiwon, Chungnam 339-700, Korea

Kyu-Hwang Yeon
Department of Physics, College of Natural Science, Chungbuk National University, Cheonju, Chungbuk 361-763, Korea
(Received 1 December 2006; revised manuscript received 22 February 2007; published 17 July 2007)

Exciton dynamics, eigenstates, and eigenenergies of nanochains consisting of closely spaced nanocrystals (NC's) are studied with a simple resonant energy transfer model. The simple NC chains considered are a linear chain, a circular chain, and a chain with a ring. The eigen-wave-functions and eigenenergies are obtained for the NC chains, and the exciton population dynamics in each system is analyzed by obtaining the diagonal elements of the density matrix for a specified initial excitation of an NC. The correlation between opposite NC's in the ring of the NC chain with a ring is considered, as well. In the NC nanochains with the resonant energy transfer model, the energy transfer via resonance dipole-dipole interaction generates propagating exciton waves which interfere with each other.

DOI: 10.1103/PhysRevB.76.035321 PACS number(s): 73.23.−b, 71.35.−y, 78.67.Bf

I. INTRODUCTION

Exciton dynamics, eigenstates, and eigenenergies have been studied enormously in the field of molecular aggregates and molecular crystals, especially in the field of photosynthesis.[1] Along with the development of the nanotechnology, artificial molecular aggregates which are composed of nanocrystals (NC's) or nanoparticles (NP's) are considered to be constructed.[2] Thus even though the exciton hopping in photosynthetic systems and molecular aggregates has been studied enormously, the phenomena of the energy transport in nanostructures have been revived due to the increase of the controlling skill of the nanostructure. Among lots of geometric structures of NC or NP aggregates, the simplest systems have been studied by many research groups.[3–7] Maier *et al.* have studied the quantum devices such as NP chain arrays for the control of the excitation in quantum nanostructures.[3] In such systems, recently much attention has been aroused especially on the study of quantum transport in an NP array.[4] That is, the electronic transport through a quantum dot array containing an arbitrary number of quantum dots connected in a series by tunnel coupling has been well studied.[5–8] In addition to the real charge transport by tunnel coupling, the electromagnetic energy transfer in a NP array has been also studied for nanodevices of near field wave guide.[3,9] In their study, the excitation hopping in a linear array of NP aggregate was considered to be resulted from the energy transfer via resonance dipole-dipole interaction (RDDI).

We are interested in the question of how to understand the wave properties of the excitation transport in a simple NC or NP array, where NC's or NP's are considered to be coupled by RDDI.[1,10] Then, in this study, the general feature of the exciton statics and dynamics in three simple nanochain systems consisting of closely spaced semiconductor nanocrystals is considered. In order to obtain the excitation energy transfer probability, a simple dipole-dipole coupling model is employed.[11] The simple NC chain systems considered are a linear chain, a circular chain, and a chain with a ring. In the chain, the energy transfer via RDDI generates propagating exciton waves which reflect from ends or nodes, split at nodes in the chains, and interfere with themselves. A simple linear NC chain (LNC) is considered to observe the effect of open ends in the chain. In comparison, a circular NC chain (CNC) is considered to observe the effect of the structure without ends. That means, in the case of CNC, the effect of the reflection from open ends in an LNC is removed. Finally an NC chain with a ring (NCR) is considered for observing the effect of the interference between the linear chain part and the ring part, where the ring can be considered as the part of two arms in a Mach-Zehnder interferometer, in some aspects. In order to analyze exciton statics in the simple systems, first of all, the eigen-wave-functions and eigenenergies are obtained for the three NC chains in the next section. The simple model of the exciton hopping is also briefly described in the next section. Based on the eigen-wave-functions and eigenenergies obtained in Sec. II, the analysis of the dynamic properties, i.e., the excitation propagation follows in Sec. III. We discuss the results obtained in Secs. II and III, and summarize briefly in Sec. IV.

II. EIGENSTATES AND EIGENENERGIES

In a nanocrystal aggregate when real charge transport between NC's by surface passivation of NC's is inhibited, an excited NC interacts with other NC's via both longitudinal field and transverse field. Through interacting with the field, the excitation energy of the NC is transported by the resonant dipole-dipole interaction between the virtual electromagnetic field generated by the transition dipole in an excited donor NC and the polarization of a ground-state acceptor NC. We employ a simple model for several NC chains consisting of NC arrays as shown in Fig. 1, where each dot represents NC and each line indicates dipole-dipole coupling. The Hamiltonian of the NC aggregate is given by

$$\hat{H} = \frac{1}{2}\sum_i \omega_i \sigma_i^z + \sum_{i \neq j} J_{ij} \sigma_i^\dagger \sigma_j, \tag{1}$$

where ω_i is the excitonic energy of the ith NC and J_{ij} is the Coulomb dipole-dipole coupling between ith and jth NC's.

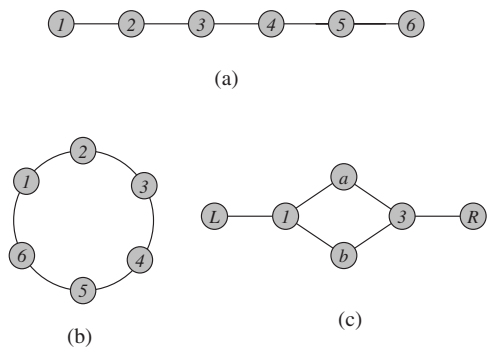

FIG. 1. Nanocrystal chains. (a) Linear NC chain (LNC), (b) circular NC chain (CNC), (c) NC chain with a nanoring (NCR).

Here σ_i^z, $\sigma_i^\dagger$, and σ_i are the Pauli operators which describe inversion, excitation, and deexcitation of the ith NC, respectively. In this study, we consider an NC aggregate with inter-NC separation R to be much shorter than the wavelength of the excitonic transition energy, where the main channel of the exciton hopping is RDDI and retarded interaction is ignored. For simplicity we also consider the single excitation in an NC, as well. The dipole-dipole coupling energy without the orientational factor is

$$J_{ij} = \kappa_{ij} \frac{\mu_i \mu_j}{\epsilon R_{ij}^3}, \tag{2}$$

where μ_i is the transition dipole moment of the ith NC, R_{ij} is the inter-NC distance, ϵ is the dielectric constant of the surrounding medium, and κ_{ij} is an angular dipole orientation factor.

For simplicity we consider the single excitation in which only one NC is initially excited and all other NCs are initially unexcited. There are N states which span the subspace of interest for the aggregate of N nanocrystals. The basis state represented by $|j\rangle$ is defined as only the jth NC is excited and all other NC's are unexcited. Then the wave function of the Hamiltonian $\hat{H}$ can be written as

$$|\psi(t)\rangle = \sum_{j=1}^{N} c_j(t)|j\rangle. \tag{3}$$

First let us consider the eigenstates and eigenenergies of a simple LNC shown in Fig. 1(a) for the Hamiltonian of Eq. (1) with only nearest-neighbor interactions. When all NC's are identical with equi-interdistance and J_{ij} is equal to J for all NC pairs, the Hamiltonian of the LNC is expressed as

$$\hat{H} = \begin{pmatrix} \omega & J & 0 & 0 & 0 & 0 \\ J & \omega & J & 0 & 0 & 0 \\ 0 & J & \omega & J & 0 & 0 \\ 0 & 0 & J & \omega & J & 0 \\ 0 & 0 & 0 & J & \omega & J \\ 0 & 0 & 0 & 0 & J & \omega \end{pmatrix}, \tag{4}$$

from which the stationary exciton state $|\phi_m\rangle$ of the chain is given by

$$|\phi_1\rangle = \frac{1}{\sqrt{\zeta_1}} \begin{pmatrix} 1 \\ \eta_1 \\ \eta_1^2 - 1 \\ \eta_1^2 - 1 \\ \eta_1 \\ 1 \end{pmatrix}, \quad |\phi_2\rangle = \frac{1}{\sqrt{\zeta_2}} \begin{pmatrix} 1 \\ -\eta_2 \\ \eta_2^2 - 1 \\ \eta_2^2 - 1 \\ -\eta_2 \\ 1 \end{pmatrix},$$

$$|\phi_3\rangle = \frac{1}{\sqrt{\zeta_3}} \begin{pmatrix} 1 \\ -\eta_3 \\ \eta_3^2 - 1 \\ \eta_3^2 - 1 \\ -\eta_3 \\ 1 \end{pmatrix}, \quad |\phi_4\rangle = \frac{1}{\sqrt{\zeta_4}} \begin{pmatrix} -1 \\ -\eta_4 \\ -\eta_4^2 + 1 \\ \eta_4^2 - 1 \\ \eta_4 \\ 1 \end{pmatrix},$$

$$|\phi_5\rangle = \frac{1}{\sqrt{\zeta_5}} \begin{pmatrix} -1 \\ \eta_5 \\ -\eta_5^2 + 1 \\ \eta_5^2 - 1 \\ -\eta_5 \\ 1 \end{pmatrix}, \quad |\phi_6\rangle = \frac{1}{\sqrt{\zeta_6}} \begin{pmatrix} -1 \\ \eta_6 \\ -\eta_6^2 + 1 \\ \eta_6^2 - 1 \\ -\eta_6 \\ 1 \end{pmatrix}, \tag{5}$$

with the energy eigenvalues λ_m,

$$\lambda_m = \omega + \eta_m J, \quad m = 1, \ldots, 6, \tag{6}$$

where

$$\eta_1 = \frac{7 + \alpha + \alpha^2}{3\alpha},$$

$$\eta_2 = \frac{7 - 2\alpha + \alpha^2 + (7 - \alpha^2)\sqrt{3}i}{6\alpha},$$

$$\eta_3 = \frac{7 - 2\alpha + \alpha^2 - (7 - \alpha^2)\sqrt{3}i}{6\alpha},$$

$$\eta_4 = \frac{7 - \beta + \beta^2}{3\beta},$$

$$\eta_5 = \frac{7 + 2\beta + \beta^2 + (7 - \beta^2)\sqrt{3}i}{6\beta},$$

$$\eta_6 = \frac{7 + 2\beta + \beta^2 - (7 - \beta^2)\sqrt{3}i}{6\beta},$$

$$\zeta_j = 4 - 2\eta_j^2 + 2\eta_j^4, \quad j = 1, \ldots, 6, \tag{7}$$

and

$$\alpha = \left(\frac{7}{2}\right)^{1/3} (-1 + 3\sqrt{3}i)^{1/3},$$

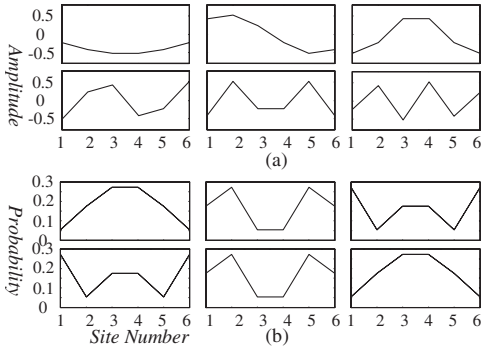

FIG. 2. Eigenstates for the linear NC chain. (a) Eigen-wave-functions and (b) their corresponding population probabilities.

$$\beta = \left(\frac{7}{2}\right)^{1/3}(1 + 3\sqrt{3}i)^{1/3}. \tag{8}$$

The above eigenvectors and eigenenergies are obtained from the eigenvalue equation $\hat{H}|\phi_m\rangle = \lambda_m|\phi_m\rangle$. The eigenvectors of Eq. (5) are shown in Fig. 2(a), where the eigenenergy of each eigenvector decreases from the upper leftmost to the lower rightmost of the six eigenfunctions. Each plot of Fig. 2(b) is the excitation population probability corresponding to each eigen-wave-function of Fig. 2(a).

For an LNC of Fig. 1(a), when both ends of the chain are connected via RDDI coupling with J, a nanochain ring of Fig. 1(b) is obtained. Then the Hamiltonian of a CNC of identical NC's with equi-interdistance is expressed as

$$\hat{H} = \begin{pmatrix} \omega & J & 0 & 0 & 0 & J \\ J & \omega & J & 0 & 0 & 0 \\ 0 & J & \omega & J & 0 & 0 \\ 0 & 0 & J & \omega & J & 0 \\ 0 & 0 & 0 & J & \omega & J \\ J & 0 & 0 & 0 & J & \omega \end{pmatrix}. \tag{9}$$

With the Hamiltonian, the eigenstates of the circular aggregate of NC's with only nearest-neighbor interactions are expressed as

$$|\phi_1\rangle = \frac{1}{\sqrt{6}}\begin{pmatrix} 1 \\ 1 \\ 1 \\ 1 \\ 1 \\ 1 \end{pmatrix}, \quad |\phi_2\rangle = \frac{1}{\sqrt{6}}\begin{pmatrix} 1 \\ -1 \\ 1 \\ -1 \\ 1 \\ -1 \end{pmatrix}, \quad |\phi_3\rangle = \frac{1}{2}\begin{pmatrix} -1 \\ 1 \\ 0 \\ -1 \\ 1 \\ 0 \end{pmatrix},$$

$$|\phi_4\rangle = \frac{1}{2}\begin{pmatrix} -1 \\ 0 \\ 1 \\ -1 \\ 0 \\ 1 \end{pmatrix}, \quad |\phi_5\rangle = \frac{1}{2}\begin{pmatrix} -1 \\ -1 \\ 0 \\ 1 \\ 1 \\ 0 \end{pmatrix}, \quad |\phi_6\rangle = \frac{1}{2}\begin{pmatrix} 1 \\ 0 \\ -1 \\ -1 \\ 0 \\ 1 \end{pmatrix}, \tag{10}$$

that is,[1,12]

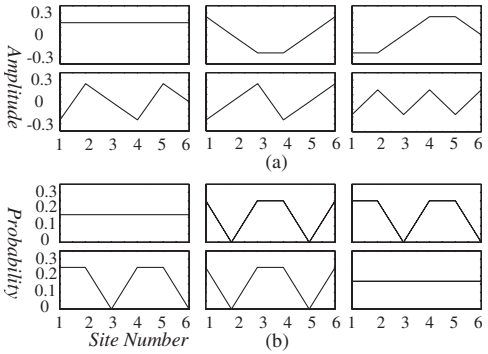

FIG. 3. Eigenstates for the circular NC chain. (a) Eigen-wave-functions and (b) their corresponding population probabilities.

$$|\phi_m\rangle = \frac{1}{\sqrt{N}}\sum_{n=1}^{N} e^{i2nm\pi/N}|n\rangle, \tag{11}$$

which results from the property of the N-fold rotational symmetry of the Hamiltonian Equation (9). This property requires periodicity, $|\phi_m\rangle = |\phi_{m+N}\rangle$, i.e., the periodic boundary condition. Whereas, due to the absence of the rotational symmetry, periodic boundary condition is not implemented in obtaining eigenfunctions of the Hamiltonian equations (4) and (14), where the eigenfunctions are chosen to form on an orthonormal basis. The corresponding eigenvalues λ_m are

$$\lambda_m = \{\omega - 2J, \omega - J, \omega - J, \omega + J, \omega + J, \omega + 2J\}, \tag{12}$$

in mathematical form,

$$\lambda_m = \omega + 2J\cos\frac{2\pi m}{N}, \quad m = 1,2,\ldots,N. \tag{13}$$

For the CNC of six identical two-level NC's with equidistance, there are two degeneracies as shown in Eqs. (10) and (12). The degeneracy comes from the rotational symmetry of the ring. The eigenvectors of Eq. (10) are shown in Fig. 3, where (a) is for the amplitude of each eigen-wave-function and (b) is for the excitation population probability of each eigen-wave-function in (a).

Now let us consider a short NCR, i.e., an NC chain with two arms as shown in Fig. 1(c). In the figure, sites a and b are considered as two paths of the chain ring at nodes 1 and 3. Only the interactions between the nearest neighbors are considered, and no interaction between different paths is assumed, that is, $J_{ab}=0$. In this case, the Hamiltonian is simply expressed as

$$\hat{H} = \begin{pmatrix} \omega & J_R & 0 & 0 & 0 & 0 \\ J_R & \omega & J_a & J_b & 0 & 0 \\ 0 & J_a & \omega & 0 & J_a & 0 \\ 0 & J_b & 0 & \omega & J_b & 0 \\ 0 & 0 & J_a & J_b & \omega & J_R \\ 0 & 0 & 0 & 0 & J_R & \omega \end{pmatrix}, \tag{14}$$

where i in Eq. (1) is $i=L,1,a,b,3,R$. When NC's are identical and RDDI couplings are given by $J_{L1}=J_{3R}=J_R$, J_{1a}

$=J_{a3}=J_a$, and $J_{1b}=J_{b3}=J_b$, the eigenvectors of the NC chain with a nanoring are given by

$$|\phi_1\rangle = \frac{J_b}{L}\begin{pmatrix} \frac{J_R}{2J_b} \\ -\frac{L}{2J_b} \\ \frac{J_a}{J_b} \\ 1 \\ -\frac{L}{2J_b} \\ \frac{J_R}{2J_b} \end{pmatrix}, \quad |\phi_2\rangle = \frac{1}{2}\begin{pmatrix} -1 \\ 1 \\ 0 \\ 0 \\ -1 \\ 1 \end{pmatrix},$$

$$|\phi_3\rangle = \frac{J_a}{\sqrt{2J_a^2+J_R^2}}\begin{pmatrix} 1 \\ 0 \\ -\frac{J_R}{J_a} \\ 0 \\ 0 \\ 1 \end{pmatrix}, \quad |\phi_4\rangle = \frac{J_a}{\sqrt{J_a^2+J_b^2}}\begin{pmatrix} 0 \\ 0 \\ -\frac{J_b}{J_a} \\ 1 \\ 0 \\ 0 \end{pmatrix},$$

$$|\phi_5\rangle = \frac{1}{2}\begin{pmatrix} -1 \\ -1 \\ 0 \\ 0 \\ 1 \\ 1 \end{pmatrix}, \quad |\phi_6\rangle = \frac{J_b}{L}\begin{pmatrix} \frac{J_R}{2J_b} \\ \frac{L}{2J_b} \\ \frac{J_a}{J_b} \\ 1 \\ \frac{L}{2J_b} \\ \frac{J_R}{2J_b} \end{pmatrix}, \tag{15}$$

with eigenvalues

$$\lambda_m = \{\omega - L, \omega - J_R, \omega, \omega, \omega + J_R, \omega + L\}, \tag{16}$$

where

$$L = (2J_a^2 + 2J_b^2 + J_R^2)^{1/2}. \tag{17}$$

The eigenvectors Eq. (15) are shown in Fig. 4(a) when $J_R=J_b=J_a=J$. Figure 4(b) shows the corresponding exciton population probability to each eigenvector in Fig. 4(a).

III. EXCITON DYNAMICS

Let us now consider the exciton dynamics in three simple NC chain systems of Fig. 1. For a given Hamiltonian, the density operator $\hat{\rho}(t)$ in Heisenberg representation is written as

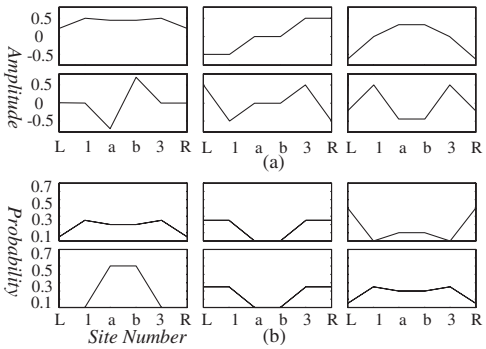

FIG. 4. Eigenstates for the NC chain with a nanoring. (a) Eigenwave-functions and (b) their corresponding population probabilities.

$$\hat{\rho}(t) = \exp(i\hat{H}t)\hat{\rho}(0)\exp(-i\hat{H}t), \tag{18}$$

where $\hat{\rho}(0)$ is the initial density matrix. The diagonal elements of the density matrix $\hat{\rho}(t)$ show the dynamics of the exciton population, and the off-diagonal matrix elements of $\hat{\rho}(t)$ carry the information of the dynamical correlation of the excitations between two NC's. When $\hat{H}$ is diagonalizable, i.e., if it is possible to find U such that $H=UDU^{-1}$ and to define

$$\exp(H) \equiv U\exp(D)U^{-1}, \tag{19}$$

where D is a diagonalized matrix and

$$U = (\hat{e}_1, \ldots, \hat{e}_6). \tag{20}$$

Here $\hat{e}_j$ is j th eigenvector $(=|\psi_j>)$ of the Hamiltonian $\hat{H}$, then the density matrix Eq. (18) is expressed as

$$\hat{\rho}(t) = \sum_{\alpha,\gamma} e^{i(\lambda_\alpha - \lambda_\gamma)t} U|\alpha\rangle\langle\alpha|\rho_U|\gamma\rangle\langle\gamma|U^{-1}, \tag{21}$$

where λ_j is j th eigenvalue of the Hamiltonian $\hat{H}$ corresponding to the j th eigenstate $|\psi_j>$, and $\rho_U=U^{-1}\hat{\rho}(0)U$. Then the matrix element of the density matrix is given by

$$\rho_{mn}(t) = \sum_{\alpha,\gamma} e^{i(\lambda_\alpha - \lambda_\gamma)t} U_{m\alpha}(\rho_U)_{\alpha\gamma}(U^{-1})_{\gamma m}. \tag{22}$$

Here since the diagonal elements $\rho_{nn}(t)$ for CNC come from the property of the N-fold rotational symmetry of the Hamiltonian Eq. (9) they satisfy the periodicity, $\rho_{nn}(t)=\rho_{(n+N)(n+N)}(t)$, i.e., the periodic boundary condition. Whereas, due to the absence of the rotational symmetry of the Hamiltonians Eqs. (4) and (14), periodic boundary condition is not implemented in obtaining the diagonal elements $\rho_{nn}(t)$ for LNC and NCR, where they are determined to satisfy the Dirichlet boundary condition for a given initial condition $\rho(0)$.

Now for a specially prepared initial excitation $\hat{\rho}(0)$, substituting eigenvectors and eigenenergies obtained in Sec. II into Eq. (22), we can get the dynamics of the excitation population of n th NC, i.e., $\rho_{nn}(t)$ for three simple nanochains of Fig. 1. First, for a linear nanochain of Fig. 1(a), when the first NC of the chain is initially excited, i.e., $\rho_{kl}(0)=\delta_{k1}\delta_{k1}$,

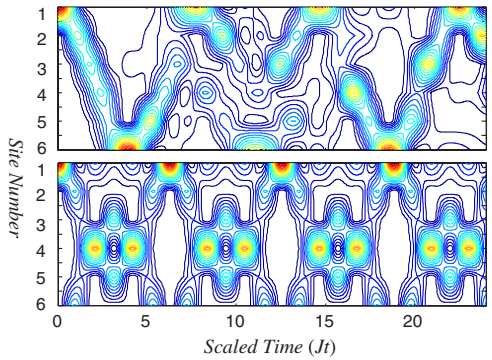

FIG. 5. (Color online) Contour plot of the probability of exciton population for (a) LNC and (b) CNC when $\rho_{kl}(0)=\delta_{kl}\delta_{kL}$. Vertical axis indicates the site label, horizontal axis is scaled time Jt, and the contour represents the exciton population, where the contour line with warmer color indicates higher population than the line with colder color.

the diagonal matrix elements $\rho_{nn}(t)$ are obtained by substitution of eigenvectors and eigenenergies of Eqs. (5) and (6) into Eq. (22), and they are shown as the upper picture in Fig. 5. In the figures, vertical axis indicates the site label of NC's in Fig. 1, horizontal axis is scaled time Jt, and the contour represents the exciton population, where the contour line with hotter color indicates higher population than the line with colder color. In case of the linear nanochain, the matrix elements $\rho_{nn}(t)$ are not given mathematically in simple analytical form, thus the plots of exciton populations were given by numerical evaluation of Eq. (22). Similarly, from Eqs. (10), (12), and (22) the exciton populations are obtained for a CNC of Fig. 1(b) and they are shown as the lower picture in Fig. 5.

For an NCR of Fig. 1(c), the matrix elements of $\hat{\rho}(t)$ which represent the excitation dynamics in the NCR are expressed in simple mathematical forms on simplified conditions. When NC's are identical, $J_{L1}=J_{3R}=J_R$, $J_{12a}=J_{2a3}=J_a$, and $J_{12b}=J_{2b3}=J_b$ on the initial excitation of $\rho_{kl}(0)=\delta_{kl}\delta_{kL}$, from Eqs. (15), (16), and (22), the diagonal elements of the density matrix are expressed as follows:

$$\rho_{LL}(t)=\frac{1}{L^4}\left(L^2\cos^2\frac{J_Rt}{2}-J_R^2\sin^2\frac{Lt}{2}\right)^2, \tag{23}$$

$$\rho_{11}(t)=\frac{1}{4L^2}(L\sin J_Rt+J_R\sin Lt)^2, \tag{24}$$

$$\rho_{aa}(t)=\frac{4J_a^2J_R^2}{L^4}\sin^4\frac{Lt}{2}, \tag{25}$$

$$\rho_{bb}(t)=\frac{4J_b^2J_R^2}{L^4}\sin^4\frac{Lt}{2}, \tag{26}$$

$$\rho_{33}(t)=\frac{1}{4L^2}(L\sin J_Rt-J_R\sin Lt)^2, \tag{27}$$

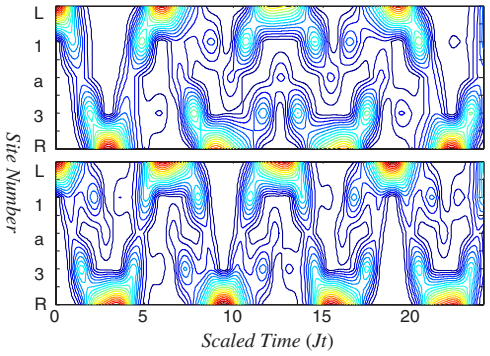

FIG. 6. (Color online) Contour plot of the probability of exciton population for the initial excitation of NC at L. They show the propagation of the exciton hopping through the arm a. The upper is for $J_a=J$ and the lower is for $J_a=2J$.

$$\rho_{RR}(t)=\frac{1}{L^4}\left(L^2\sin^2\frac{J_Rt}{2}-J_R^2\sin^2\frac{Lt}{2}\right)^2. \tag{28}$$

They are shown in Fig. 6. The upper and lower are plots of the propagations of the excitation through arm a for $J_a=1$ and $J_a=2$, respectively. The excitation population in the ring part only is also shown in Fig. 7. The upper is for $J_a=1$ and the lower is for $J_a=2$.

In order to analyze the correlation effect of the excitation between NC's in the ring part of Fig. 1(c), we consider the off-diagonal elements of the density matrix. The off-diagonal element between site a and b in the ring, $\rho_{ab}(t)$, is given by

$$\rho_{ab}(t)=\frac{4J_aJ_bJ_R^2}{L^4}\sin^4\frac{Lt}{2}, \tag{29}$$

which couples to the diagonal elements $\rho_{aa}(t)$, $\rho_{bb}(t)$ and shows the feature of the interference between two arms and its period is a function of the variable L. Whereas, the off-diagonal element between site 1 and 3 in the ring, $\rho_{13}(t)$, is obtained as

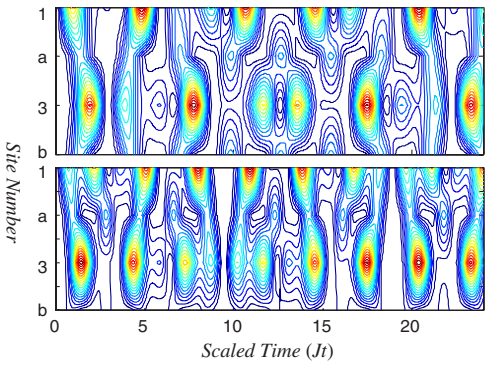

FIG. 7. (Color online) Contour plot of the probability of exciton population of the ring part only in NCR for $J_a=J$ and $J_a=2J$ when the NC at L is initially excited.

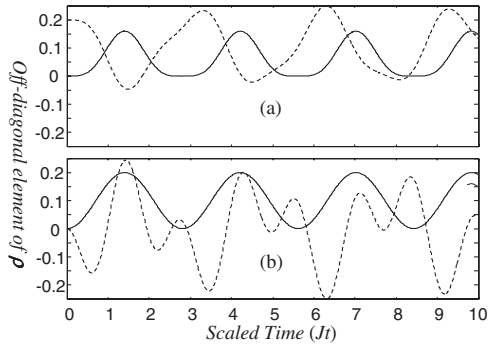

FIG. 8. The off-diagonal elements $\rho_{ab}(t)$ (solid line) and $\rho_{13}(t)$ (dashed line) for NCR. (a) is for the initial excitation of NC at L and (b) is for the initial excitation of NC at 1.

$$\rho_{13}(t) = \frac{1}{4L^2}(L^2 \cos^2 J_R t - J_R^2 \cos^2 Lt), \tag{30}$$

in which the effect of both ends in the chain are included as the variables J_R and L. They are shown in Fig. 8(a). The solid line is for $\rho_{ab}(t)$ and the dashed line is for $\rho_{13}(t)$. As a reference, for the initial excitation $\rho_{kl}(0) = \delta_{kl}\delta_{k1}$, the off-diagonal elements $\rho_{ab}(t)$ and $\rho_{13}(t)$ are given by

$$\rho_{ab}(t) = \frac{J_a J_b}{L^2} \sin^2 \frac{Lt}{2} \tag{31}$$

and

$$\rho_{13}(t) = \tfrac{1}{8}(\cos 2Lt - \cos 2J_R t), \tag{32}$$

respectively, and they are plotted in Fig. 8(b). The solid line and dashed line are for $\rho_{ab}(t)$ and $\rho_{13}(t)$, respectively, as well.

IV. DISCUSSION AND CONCLUSION

In order to study the wave properties of the excitation transport in a simple NC chain where NCs are coupled by RDDI, exciton eigen-wave-functions and exciton dynamics for three simple NC chains (a linear chain, a circular chain, and a chain with a ring) were obtained. In the chain, the energy transfer from an initially excited NC to other NCs via RDDI generates propagating exciton waves which reflect from ends or nodes, split at nodes in the chains, and interfere with themselves. A simple linear NC chain was considered to observe the effect of open ends. In comparison, a circular NC chain was considered to see the effect without ends, i.e., the effect of the reflection from the open end in a simple linear NC chain is removed. Finally an NC chain with a ring was considered for observing the effect of the interference between the linear chain part and the ring part.

The time evolution of each exciton state $\rho(t)$ after an initial excitation of the first NC in each chain has been analyzed in Sec. III. The initial excitation of an NC in a chain could be obtained via optical pumping through a nanoscale tip of an optical fiber. The time evolution of the excitation of an NC in the chain after an initial excitation of the first NC shows a specific feature of coherent oscillations due to dipole-dipole coupling with neighboring identical NCs. Since the typical coupling energy between close NCs is $J \sim 0.1$ meV for the transition dipole moment $\mu \sim 10$ Debye and the inter-NC distance $R \sim 100$ Å, the oscillation period is ~ 10 ps which is much faster than radiative decay.[13–15] The time evolution could be probed optically through the irreversible Förster energy transfer from the excited probed smaller NC whose low-lying exciton state is resonant to a high-lying exciton state of the probing NC attached at the end of a nanoscale tip of an optical fiber. The existence of the probing NC would affect the coherent oscillations in each chain, but may do so only weakly.

The described eigenstates, eigenenergies, and exciton dynamics of the three NC chains in Secs. II and III assumed perfect structure and neglected any kind of disorder. One-dimensional quantum-mechanical hopping, however, is extremely sensitive to the disorder.[16–18] Since the one-dimensional localization length is of the order of the lattice spacing, it is crucial to consider the disorder effects for the NC chains. In general, the disorder broadens the energy spectrum and shortens the effective exciton delocalization length. The disorder can be classified into two types; the diagonal disorder and the off-diagonal disorder which are consequences of structural inhomogeneities of the NC chains and the local excitation energies of each NC. The robustness of the results obtained in Secs. II and III with respect to the randomness in the site energies $\Delta\omega_j$ and in the hopping elements ΔJ_{ij} has been considered by numerical modeling of the randomness for three NC chains.

A. Eigenstates and eigenenergies

In the figures of eigenfunctions, Figs. 2–4 (a)'s are eigen-wave-functions and (b)'s are their corresponding exciton population probabilities. In each set of eigenvectors, the eigenenergy of each eigenvector decreases from the upper leftmost to the lower rightmost. In the plots of eigenvectors, it is seen that the lower the spatial variation of the eigen-wave-function is, the higher the eigenenergy is. For the same single exciton energy ω for all NC's, the eigenenergies of LNC measured from ω are $(-1.80, -1.25, -0.45, 0.45, 1.25, 1.80)$ in units of J. In the same units, those for CNC and NCR are $(-2, -1, -1, 1, 1, 2)$ and $(-2.24, -1, 0, 0, 1, 2.24)$, respectively. It is seen that the more the number of coupling is, the broader the shift is, as expected. We see also that there is no degeneracy in case of LNC due to the absence of symmetry. Whereas there are two degeneracies in the eigenstates of CNC, which come from the rotational symmetry of the chain ring. The (second-third) and the (fourth-fifth) pairs from the upper leftmost have the same eigenenergy in Fig. 4. In the case of NCR, there is one degeneracy with eigenenergy ω due to the symmetry of the two sites a and b (the indistinguishability of the arm a and b for the propagation of the excitation). The third and the fourth from the upper leftmost has the same eigenenergy in Fig. 4.

Now for the analysis of the effects of the ring in the chain of Fig. 1(c), we reexpress the eigen-wave-functions of the ring part only as

$$|\phi_1\rangle \sim \begin{pmatrix} -\frac{L}{2J_b} \\ \frac{J_a}{J_b} \\ -\frac{L}{2J_b} \\ 1 \end{pmatrix}, \quad |\phi_2\rangle \sim \begin{pmatrix} 1 \\ 0 \\ -1 \\ 0 \end{pmatrix}, \quad |\phi_3\rangle \sim -\begin{pmatrix} 0 \\ \frac{J_R}{J_a} \\ 0 \\ 0 \end{pmatrix},$$

$$|\phi_4\rangle \sim \begin{pmatrix} 0 \\ -\frac{J_b}{J_a} \\ 0 \\ 1 \end{pmatrix}, \quad |\phi_5\rangle \sim \begin{pmatrix} -1 \\ 0 \\ 1 \\ 0 \end{pmatrix}, \quad |\phi_6\rangle \sim \begin{pmatrix} \frac{L}{2J_b} \\ \frac{J_a}{J_b} \\ \frac{L}{2J_b} \\ 1 \end{pmatrix}. \tag{33}$$

For comparison, a circular NC chain ring composed of four NC's is considered. In that case, the eigenstates and their eigenenergies are given by

$$|\phi_1\rangle = \frac{1}{2}\begin{pmatrix} 1 \\ 1 \\ 1 \\ 1 \end{pmatrix}, \quad |\phi_2\rangle = \frac{1}{\sqrt{2}}\begin{pmatrix} 0 \\ -1 \\ 0 \\ 1 \end{pmatrix},$$

$$|\phi_3\rangle = \frac{1}{\sqrt{2}}\begin{pmatrix} -1 \\ 0 \\ 1 \\ 0 \end{pmatrix}, \quad |\phi_4\rangle = \frac{1}{2}\begin{pmatrix} 1 \\ -1 \\ 1 \\ -1 \end{pmatrix}, \tag{34}$$

and

$$\lambda = \{\omega + 2J, \omega, \omega, \omega - 2J\}, \tag{35}$$

respectively. As required when $J_R=0$ and $J_a=J_b=J$, i.e., when the ring in NCR is separated from the main chain, eigenstates of the ring of Eq. (33) for NCR correspond to those of Eq. (34) for a circular ring with four NC's. Now when $J_R \neq 0$, two modes $|\phi_2\rangle$ and $|\phi_5\rangle$ in Eq. (33) remain the same as $|\phi_3\rangle$ or $|\phi_2\rangle$ in Eq. (34), whereas three modes $|\phi_1\rangle$, $|\phi_4\rangle$, and $|\phi_6\rangle$ in Eq. (33) are modified. And a new mode $|\phi_3\rangle$ in Eq. (33) appears. Thus from comparing Fig. 4(a) with Fig. 3(a) we can see that the shape of the wave function for the ring part 1-*a*-3-*b* of each wave function in Fig. 4(a) is very similar to that of the corresponding wave function in Fig. 3(a). Moreover since NCR has a linear part, we see that the shape of the wavefunction for the linear part *L*-1-*a*(or *b*)-3-*R* of each wave function in Fig. 4(a) is very similar to that of the corresponding wave function in Fig. 2(a), as expected.

B. Exciton dynamics

In an NC chain, the energy transfer via RDDI between nearly identical NCs generates propagating exciton waves which interfere with themselves. Our study has focused on the excitonic state in an NCR of Fig. 1(c). For comparison, an LNC of Fig. 1(a) and a CNC of Fig. 1(b) were considered to observe the effect of open ends and the effect of the structure without open ends, respectively. In the case of CNC, there is no effect of the reflection from ends due to the absence of open ends compared to the case of LNC. Whereas since an NCR has the character of both LNC and CNC, it is expected to observe the effect of the interference between the linear part and the ring part of the chain.

First in the case of the LNC of Fig. 1(a), the excitonic wave propagates from the initially excited NC at site 1 to the other NCs as shown in the upper picture of Fig. 5. In the figures, vertical axis indicates the site label of NC's in Fig. 1, horizontal axis is scaled time Jt, and the contour represents the exciton population, where the contour line with hotter color indicates higher population than the line with colder color. The propagation of the excitation from the initially excited first NC to the NC at the opposite end in the linear chain is shown as a ridge from 1 to 6 in the figure. During the propagation, the partially reflected excitonic wave from each lattice point interferes with each other and the form of a bulge around the central part (site 3) of the chain at time around $Jt \sim 4$ appears in the figure. The reflected excitonic wave from 6 interferes with the incoming excitonic wave (mainly from 3) to 6, and its propagation from 6 to 3 slows down a bit. However its propagation time from 6 back to 1 is shorter than that from the initially excited NC 1 to 6 due to the constructive interference with the excitonic wave (mainly) from 3. A ridge starting from 6 to 1 is divided at time around $Jt \sim 7.5$ (at 2) into two, one from 3 to 6, the other from 1 to 4, which comes from the interference of the excitonic wave propagating from 6 to 1 with both re-reflected from 6 and reflected from 1. We can see clearly the effect of open end, i.e., reflections of excitonic waves from 1 and 6, and interferences between them.

Next, in case of CNC of Fig. 1(b) the excitonic wave propagation from the initially excited NC at site 1 to other NC's is shown in the lower picture in Fig. 5. Considering that sites 1 and 6 are connected via RDDI with coupling strength J, there is no such end effect as reflections in the case of LNC. The excitation population mainly oscillates between sites 1 and 4. And due to the destructive interference, the excitation population at sites around 2 and 6 is relatively rare. The oscillation of the exciton population in CNC comes from the fact that there are two rotational paths for the excitation transport. Two exciton waves traveling in opposite direction which are separated from the initially excited NC at 1 interfere with each other. In CNC the initially excited energy at 1 moves to 2, 6, and partially back to 1 symmetrically, next transfers to 3, 5, and partially back to 2, 6, and eventually moves to 4, where the propagation from 1 through 2, 3 constructively interferes with the propagation from 1 through 6, 5. The initial energy in the NC at 1 is not completely transferred to 4 as seen from the crest around time $Jt \sim 2$. The energy transferred to 4 moves back completely to 1 at around time $Jt \sim 6$. Due to the interference of two excitonic waves propagating clockwise and counterclockwise, the initially excited energy of the NC at 1 is not completely transferred to the NC at 4 compared to the case of LNC.

Finally, the exciton dynamics of NCR is shown in Fig. 6. The upper and the lower are the excitonic wave propagations through arm a of Fig. 1(c), for $J_a=J$ and $J_a=2J$, respectively. In Fig. 1(c), sites a and b are two possible paths for the propagation of an excitonic wave from L to R (or from R to L), and the wave can rotate in the ring-part (1-a-3-b) in a clockwise way or in a counterclockwise way. From Figs. 6 and 7 it is seen that the propagation of the excitation transport in the case with $J_a=2J$ is a little bit faster than that in the case with $J_a=J$, as expected. When we consider only the linear part of NCR, compared to the case of LNC (the upper plot in Fig. 5), the speed of the propagation is much faster due to the existence of two paths. On the other hand, in order to compare with the case of CNC, time dependence of the exciton populations in the ring part only of NCR is plotted in Fig. 7. The upper one is for $J_a=J$ and the lower one is for $J_a=2J$. In this figure, there is the effect of the interference of the ring part with the outer part (L and R) of the NCR compared to the case of CNC (the lower plot in Fig. 5). In NCR when we consider the propagation of an exciton from the NC at L to the NC at R through the NC at a, the pattern of the propagation of the exciton is qualitatively similar to that in LNC with a slight difference due to the presence of the NC at b. And in the upper part of Fig. 7 which is for the ring-part only in NCR, the excitation energy at 1 (which is from the initially excited NC at L) is transferred to 3 through a, b (after reflection from R), next moves to a, b and eventually moves back to 1, and so on. Comparing the upper part of Fig. 7 with the lower part of Fig. 5 we see that the general feature of the exciton dynamics is qualitatively similar to that in the case of CNC, but the height of the peak of the excitation population at 1 and 3 as a function of time oscillates due to the existence of the outer-part (L and R), whereas the height of the peak of the excitation population at a and b are constant. Here we notify that the existence of the outer part enforces the complete energy transfer from NC at 1 to NC at 3 compare to the case of CNC where the initial energy is not transferred completely to the NC at the opposite side.

The off-diagonal elements $\rho_{mn}(t)$ which stand for the correlation between two NC's at sites m and n in NCR is shown in Fig. 8. The solid line and dashed line are for $\rho_{ab}(t)$ and $\rho_{13}(t)$, respectively. In the figure, (a) is for the initial excitation $\rho_{mn}(0)=\delta_{mn}\delta_{mL}$, and (b) is for the initial condition $\rho_{mn}(0)=\delta_{mn}\delta_{m1}$. The maxima of the off-diagonal elements $\rho_{ab}(t)$ and $\rho_{13}(t)$ which are for two NC's between sites opposite each other in the ring are not 1. The correlation between sites a and b, $\rho_{ab}(t)$, and sites 1 and 3, $\rho_{13}(t)$, are out of phase until nearly $Jt\sim 6$ for initial excitation $\rho_{mn}(0)=\delta_{mn}\delta_{mL}$. For the initial excitation of $\rho_{mn}(0)=\delta_{mn}\delta_{m1}$, the oscillation frequency of $\rho_{13}(t)$ is faster than that of $\rho_{ab}(t)$. Compared to the case with $\rho_{mn}(0)=\delta_{mn}\delta_{mL}$, the off-diagonal terms $\rho_{ab}(t)$ and $\rho_{13}(t)$ do not depend on J_R directly which show the effect of the reflection of the exciton. They depend on J_R through L, of course. $\rho_{ab}(t)$ is proportional to both J_a and J_b, and has the same time dependence as those of both $\rho_{aa}(t)$ and $\rho_{bb}(t)$, as expected.

C. Effect of disorder

For a highly dipole-aligned, perfectly ordered, and highly monodispersed NC aggregate, the eigenstates of the excited electronic excitation extend over the entire array, as expressed in Eqs. (5), (10), and (15). The driving force for delocalization of the electronic eigenstates over the entire array is the dipole-dipole interaction between NCs. In strongly coupled NC aggregates, electronic excitations can, in principle, be delocalized across multiple NCs. Any NC chain, however, in practice contains some amount of disorder due to the randomness in the site energies or in the hopping elements, which may severely affect the delocalization behavior of the excitonic states. In disordered NC chains, at a certain degree of disorder, a transition occurs from delocalized excitonic states to coexisting delocalized and localized states. With increasing the disorder, delocalization occurs only with respect to nearest-neighbor NCs, resulting in small clusters involving several NCs. Moreover a severe size difference between nearest neighbor NCs causes irreversible energy transfer to a larger NC (trapping) which is the so-called Förster energy transfer. The robustness of the results obtained above with respect to the diagonal disorder and the off-diagonal disorder has been considered by numerical modeling of the randomness for three NC chains. The implementation of the numerical model for a closely packed real one-dimensional NC chain was established by introducing random distributions of NC sizes and coupling energies (in which the coupling energy is given as a function of inter-NC distances, transition dipole orientations, and so on). The disorder will show inhomogeneous broadening and shift, but the spectral variation caused by the disorder was not considered here.

In order to simulate the diagonal disorder for the transition energy ω_j of the jth NC, we employed Gaussian random variables with zero mean values as the energy shift $\Delta\omega_j$ from the average transition energy ω due to NC size disparity and the environmental difference of each NC. In addition the simulation of the off-diagonal disorder was implemented by employing Gaussian random variables with zero mean value as the fluctuation ΔJ_{ij} from the average coupling energy J due to the randomness of both the inter-NC separations and the direction of the dipole vectors with respect to a fixed angle. The detail of the numerical simulation is explained as follows. A fluctuational average has been taken over a large number (2×10^3) of sets of the random variables $\Delta\omega_j$ and ΔJ_{ij}. For a small diagonal fluctuation, the excitation hopping from the initially excited NC to other NCs are shown to be highly coherent. When the fluctuation increases, the population drop of the first NC decreases, which means the increase of the degree of the localization of the excitonic state. For the fluctuation of $\Delta\omega_j$ whose variance is larger than or equal to the order of magnitude of the coupling energy J, disorder becomes important. In that case, even without fluctuations in J_{ij}, the large discrepancy of the transition energies between two NCs alone causes relatively weak but not negligible localization of the excitonic wave. Moreover, when the fluctuation is much larger than J, the first NC hardly transfers its energy to other NCs. This also means that, besides the NC size disparity, the homogeneous line broadening due to environmental temperature is an important factor to the coherent delocalization of the exciton. From the numerical simulation of the randomness of the off-diagonal disorder, we found that the off-diagonal disorder ΔJ_{ij} causes relatively weaker local-

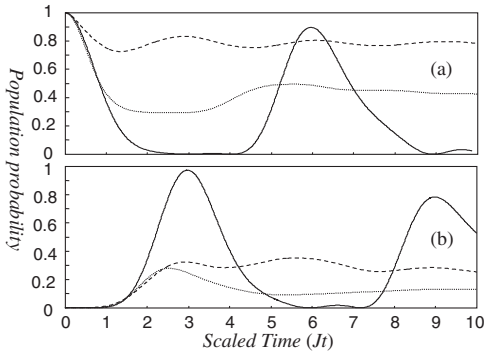

FIG. 9. The excitation population probabilities of the NCs at (a) L and R (b) in NCR when the NC at L is initially excited. Solid line is for $\Delta\omega_j=\Delta J_{ij}=0$. Dotted and dashed lines are for $\Delta J_{ij}/J=0.5$ and $\Delta\omega_j/J=0.5$, respectively. In (b), the dashed line is for $100\times\rho_{RR}(t)$.

ization of the excitonic wave than that with the same amount of the diagonal disorder. As a typical example, Fig. 9 is given to show this feature. Thus in order to observe the coherent feature of the dynamic excitonic states, smaller fluctuations of ΔJ_{ij} and $\Delta\omega_j$ than J are desired, which is more stringent for the diagonal fluctuation.

V. SUMMARY

In summary, the eigenstates and eigenenergies of three short NC chain systems consisting of closely spaced semiconductor nanocrystals were evaluated and the exciton dynamics of the NC chains were analyzed to understand the wave properties of the excitation transport in a simple NC chain. In this study we focused on the coherent coupling between NCs which was shown in a low temperature regime. In the three NC chains, the interference of exciton hopping via resonant dipole-dipole interaction was analyzed. The simple NC chain systems considered were a linear chain, a circular chain, and a chain with a ring. In the NC chains, the energy transfer via RDDI generates propagating exciton-waves which reflect from ends or nodes, split at nodes in the chains, and interfere with themselves. From the analysis of the excitonic wave propagation in an LNC, the effect of open ends is observed. In comparison, a CNC shows the effect of the periodic structure of the traveling excitonic wave due to the absence of the open ends. Whereas since an NCR has both the character of the LNC and the CNC, the effect of the interference between the linear part and the ring part of the chain is seen. In practice, however, real NC chains contain some amount of disorder due to the randomness in the site energies or in the hopping elements and the disorder severely affects the delocalization behavior of the excitonic states. Thus in order to observe the coherent feature of the dynamic excitonic states, smaller fluctuations of ΔJ_{ij} and $\Delta\omega_j$ than J are desired. That is, to support the coherent exciton dynamics, the excitation hopping should be monitored at low temperature in an NC chain which has nearly identical NCs. In practice, the initially excited energy of an NC in a chain could hop among nearly identical NCs at low temperature before a photoemission occurs from a larger probing NC to which the excitation transfers irreversibly from a probed NC in the chain.

[1] M. Chachisvilis, O. Kuhn, T. Pullerits, and V. Sundstrom, J. Phys. Chem. B **101**, 7275 (1997).
[2] J. G. Diaz, J. Planelles, W. Jaskolski, J. Aizpurua, and G. W. Bryant, J. Chem. Phys. **119**, 7484 (2003).
[3] S. A. Maier, P. G. Kik, and H. A. Atwater, Phys. Rev. B **67**, 205402 (2003).
[4] P. A. Orellana, F. Dominguez-Adame, I. Gomez, and M. L. Ladron de Guevara, Phys. Rev. B **67**, 085321 (2003).
[5] W. Z. Shangguan, T. C. Au Yeung, Y. B. Yu, and C. H. Kam, Phys. Rev. B **63**, 235323 (2001).
[6] J. X. Wang, S. Kais, F. Remacle, and R. D. Levine, J. Phys. Chem. B **106**, 12847 (2002).
[7] D. S. Novikov, M. Drndic, L. S. Levitov, M. A. Kastner, M. V. Jarosz, and M. G. Bawendi, Phys. Rev. B **72**, 075309 (2005).
[8] Y. Luo, S.-Q. Duan, W.-B. Fan, X.-G. Zao, L.-M. Wang, and B.-K. Ma, Chin. Phys. Lett. **19**, 981 (2002).
[9] M. L. Brongersma, J. W. Hartman, and H. A. Atwater, Phys. Rev. B **62**, R16356 (2000).
[10] S.-K. Hong, K.-H. Yeon, S. W. Nam, and S. Zhang, Phys. Lett. A **360**, 1 (2006).
[11] G. Juzeliunas and D. L. Andrews, Adv. Chem. Phys. **112**, 357 (2000); G. Juzeliunas and D. L. Andrews, Phys. Rev. B **49**, 8751 (1994).
[12] A. S. Davydov, *Theory of Molecular Excitons* (Plenum, New York, 1971).
[13] S. A. Crooker, J. A. Hollingsworth, S. Tretiak, and V. I. Klimov, Phys. Rev. Lett. **89**, 186802 (2002).
[14] C. B. Murray, D. J. Norris, and M. G. Bawendi, J. Am. Chem. Soc. **115**, 8706 (1993).
[15] M. L. Brongersma, J. W. Hartman, and H. A. Atwater, Phys. Rev. B **62**, R16356 (2000).
[16] S. John and T. Quang, Phys. Rev. A **52**, 4083 (1995).
[17] M. V. Artemyev, A. I. Bibik, L. I. Gurinovich, S. V. Gaponenko, and U. Woggon, Phys. Rev. B **60**, 1504 (1999).
[18] S.-K. Hong, K.-H. Yeon, S. W. Nam, and S. Zhang, J. Korean Phys. Soc. **49**, 619 (2006).